Chinese Journal of Polymer Science Vol. 35, No. 3, (2017), 434–445

Chinese Journal of Polymer Science
© Chinese Chemical Society
Institute of Chemistry, CAS
Springer-Verlag Berlin Heidelberg 2017

Effects of Zinc Oxide Nanoparticles on the Morphology and Viscoelastic Properties of Polyamide 6/Poly(butylene terephthalate) Blends

Li Wang[a, b], Zhao-xia Guo[c*] and Jian Yu[c*]

[a] *The State Key Laboratory of Chemical Resource Engineering, Beijing 100029, China*
[b] *College of Materials Science and Engineering, Beijing University of Chemical Technology, Beijing 100029, China*
[c] *Key Laboratory of Advanced Materials, Ministry of Education, Department of Chemical Engineering, Tsinghua University, Beijing 100084, China*

Abstract The morphology of polyamide 6/poly(butylene terephthalate) (PA6/PBT, 70/30, *W*/*W*) blends filled with pristine Zinc oxide (ZnO) nanoparticles and ZnO surface-modified by γ-glycidoxypropyltrimethoxysilane (K-ZnO) was investigated. The incorporation of ZnO and K-ZnO by one-step compounding both resulted in a smaller size and narrower distribution of PBT domains and the effect of ZnO was greater than K-ZnO. To reveal the underlying mechanism, two-step compounding in which ZnO or K-ZnO was premixed with PA6 or PBT was conducted and the finest morphology was achieved when mixing PA6 with premixed PBT/ZnO. Transmission electron microscopy (TEM) demonstrated that ZnO was distributed in PBT in all cases and K-ZnO was enriched at the interface except when K-ZnO was premixed with PBT. ZnO and K-ZnO caused a deterioration in the melt rheological properties of PBT, which played a dominating role in the morphological changes. In addition, the interfacial localization of K-ZnO enhanced the dynamic rheological properties of PA6/PBT blends substantially.

Keywords Zinc oxide; Polyamide 6; Poly(butylene terephthalate); Morphology; Rheology

INTRODUCTION

Polymer blending is an important route to develop polymeric materials with high performance and new functions because it can combine the advantages of the constituent virgin polymers. However, the thermodynamic immiscibility between most polymer pairs causes various types of phase-separated microstructure (morphology) during blending, which is in close relationship with the final properties of polymer blends[1]. Therefore, the tailoring of morphology is often required in pursuing optimized overall properties. Traditionally, a block or graft copolymer synthesized prior to blending or formed *in situ* is utilized as compatibilizer to obtain refined morphology.

During the past decades, extensive investigations have uncovered the potential of inorganic particles (organoclay, silica, carbon nanotubes, calcium carbonate, *etc.*) in modifying the morphology of polymer blends[2–27]. The incorporation of inorganic particles can bring about a rich diversity of morphological changes, including the refining or coarsening of morphology as well as transitions between different types of morphology. These changes have been found to be in relation to the distribution state of inorganic particles in polymer blends and their influences on the interfacial properties of polymer blends and the viscoelastic properties of different phases. Thus, the employment of inorganic particles enriches the toolbox of polymer scientists for morphology modification drastically. Regarding the refining of matrix-dispersed morphology[2–11], it has been found that the

* Corresponding authors: Zhao-xia Guo (郭朝霞), E-mail: guozx@mail.tsinghua.edu.cn
Jian Yu (于建), E-mail: yuj@mail.tsinghua.edu.cn
Received August 25, 2016; Revised September 22, 2016; Accepted October 6, 2016
doi: 10.1007/s10118-017-1905-x

location of inorganic particles can be either in the matrix phase or at the interface. For instance, Das *et al.*[4] reported the predominant distribution of clay in the matrix (POM) phase of POM/ABS (75/25, *W*/*W*) blend, resulting in a gradual decrease in number average domain diameter with increasing clay loadings. Laoutid *et al.*[17] observed a clear refinement of the morphology of PA6/PP (80/20, *W*/*W*) blend with the incorporation of hydrophobic nanosilica located mainly at the interface. We are interested in the latter case because the refining of matrix-dispersed morphology is accompanied by improved adhesion and stress transfer between different phases when inorganic particles are located at the interface.

Zinc oxide (ZnO) nanoparticles, owing to their unique optical and electronic properties, have been widely used in preparing polymer nanocomposites. The incorporation of ZnO nanoparticles can not only enhance the mechanical, crystalline, photostability and thermostability of polymeric materials, but also endow them with the functions of photocatalytic, antibacterial, UV-shielding and so on[28–38]. Despite the numerous investigations on polymer/ZnO nanocomposites, the influence of ZnO nanoparticles on the morphology of polymer blends has not been reported.

Polyamide 6 (PA6)/poly(butylene terephthalate) (PBT) blend is selected as a model system in the present study. PA6/PBT blend can combine the high barrier and mechanical strength of PA6 with good chemical/water tolerance of PBT, thus gaining widespread use in electronics, automobile and textile industries[39–41]. Traditional compatibilizing strategy for PA6/PBT blend involves the employment of small molecule compounds, oligomers and polymers with reactive functional groups that are able to react with the end groups of both PA6 and PBT, such as epoxy, oxazoline and maleic anhydride groups[39–43]. To the best of our knowledge, there are few reports on the usage of inorganic particles in tailoring the morphology of PA6/PBT blends.

Our group is committed to explore the usage of inorganic particles in morphology modification. Previously, we have demonstrated that glass fibers with different surface properties can bring about a transition from co-continuous to matrix-dispersed morphology with PA6 being matrix for PA6/PBT (45/55, *W*/*W*) blend[44]. Herein, we aimed at using ZnO nanoparticles to compatibilize PA6/PBT (70/30, *W*/*W*) blend. Pristine ZnO and ZnO surface-modified by γ-glycidoxypropyltrimethoxysilane (KH560, carrying epoxy groups that can react with the end groups of both PA6 and PBT) were utilized to distribute ZnO nanoparticles at the interface, since this structure feature is believed to bring about better compatibilizing effect. Different compounding sequences were applied and compared to help reveal the underlying mechanism for the morphological changes. The dynamic rheological properties were tested and correlated with morphology.

EXPERIMENTAL

Materials

PA6 (B3S) was obtained commercially from BASF (Malaysia). PBT was provided by Zhangjiagang HuaHui Plastic Additives Factory (China). Zinc oxide (MN6Z) with the average diameter and specific surface area being (20 ± 5) nm and (50 ± 10) m^2/g respectively was supplied by Zhoushan MingRi Nanomaterials Co. Ltd. (China). KH560 (industrial grade) was provided by Nanjing ShuGuang Chemical Factory (China).

Surface Modification of ZnO by KH560

ZnO was surface-modified by KH560, following a previously reported method[45]. Thus, 10 g of ZnO dried in a vacuum oven and 180 mL of anhydrous toluene were added into a 3-neck flask equipped with an Allihn condenser in an oil bath with mechanical stirrer. After purging with N_2, 4.5 g of KH560 in 30 mL of toluene was added dropwise using a pressure-equalizing dropping funnel in 30 min. Then the oil bath was heated to 128 °C and the reaction mixture was refluxed for 8 h. After that, the mixture was cooled to room temperature, filtered and washed with toluene for three times. Finally, the surface-modified ZnO (designated as K-ZnO) powder was subjected to Soxhlet extraction with toluene as solvent to remove any unreacted KH560, after which K-ZnO was vacuum-dried at 100 °C.

Sample Preparation

Samples were prepared by melt compounding using a torque rheometer (HAAKE PolyDrive, HAAKE Company, Germany) with a ∞-shaped mixing chamber and two counter-rotating roller blades. The screw speed, compounding temperature and time were 60 r/min, 235 °C and 6 min, respectively. The formulations and compounding sequences of all samples are given in Table 1. Three different compounding sequences were utilized, including one-step compounding, PA6 masterbatch method as well as PBT masterbatch method. The compounding conditions for the premixing step were the same to those described above.

Table 1 Formulations and compounding sequences

Designation	Formulation (weight ratio *)				Compounding sequence
	PA6	PBT	ZnO	K-ZnO	
PA6/PBT	70	30	–	–	One-step compounding
PA6/PBT/ZnO	70	30	3.09	–	
PA6/PBT/K-ZnO	70	30	–	3.09	
PA6(ZnO)/PBT	70	30	3.09	–	PA6 masterbatch method [a]
PA6(K-ZnO)/PBT	70	30	–	3.09	
PA6/PBT(ZnO)	70	30	3.09	–	PBT masterbatch method [b]
PA6/PBT(K-ZnO)	70	30	–	3.09	

[*] The formulation is expressed as the weight ratio between different components and '–' denotes the absence of a component;
[a] Mixing PBT with premixed PA6 and ZnO or K-ZnO; [b] Mixing PA6 with premixed PBT and ZnO or K-ZnO

Characterization

Field emission scanning electron microscopy (FESEM)

Samples for FESEM were prepared with two different methods to obtain an unequivocal reveal of the phase morphology. The first method was the commonly-used cryo-fracturing in liquid nitrogen and the second one was removing PA6 phase by chemical etching using formic acid (immersing samples in formic acid for 4 h, followed by centrifugation. This was repeated for 3 times). A JEOL instrument (JSM-7401F, Japan) operating at an accelerating voltage of 1 kV was used for morphology observation. The FESEM micrographs were analyzed using the Smileview software of the microscope to determine the average particle diameter (D_n). D_n is defined as $D_n = \sum_{i=1}^{n} d_i \Big/ n$, in which d_i is the diameter of the i^{th} particle.

Transmission electron microscopy (TEM)

The dispersion and distribution states of ZnO and K-ZnO in the samples were confirmed by TEM. A JEM-2010 transmission electron microscope (JEOL, Japan) operating at an accelerating voltage of 120 kV was utilized for TEM observation. Ultrathin slices were prepared with a cryoultratome (LKB model 2088; LKB-Producter AB, Bromma, Sweden) without staining.

Melt rheology

A rotational rheometer (Anton Paar-Physica MCR 301, Austria) operating with parallel plate geometry (ϕ 25 × 1 mm) in a frequency sweep mode was used for melt rheological measurements. The tests were carried out at 235 °C in N_2 atmosphere and the strain amplitude was maintained at 1%.

RESULTS AND DISCUSSION

Morphology

The FESEM micrographs of the samples prepared by one-step compounding are given in Fig. 1, with the left ones showing the cryo-fractured surfaces of the samples and the right ones presenting the PBT phases recovered after removing PA6 from the samples by chemical etching. The FESEM micrographs on the right were subjected to statistical particle size analysis using the Smileview software and the results are listed in Table 2. Hemispherical bulges and fractured surfaces of PBT domains can be observed for the PA6/PBT sample without ZnO (Fig. 1a1). Furthermore, clear interface between PA6 and PBT phases can be distinguished, which is indicative of poor interfacial adhesion. It can be seen from Fig. 1(a2) that the PBT domains existed mainly as

spherical and rod-like particles. Therefore, the PA6/PBT sample possessed the characteristic of matrix-dispersed morphology with PBT as the dispersed phase. The number average diameter of the dispersed PBT domains (D_n) was calculated to be (1.82 ± 0.57) μm. Figures 1(b) and 1(c) present the FESEM micrographs of the PA6/PBT/ZnO and PA6/PBT/K-ZnO samples. The incorporation of pristine ZnO or ZnO surface-modified by KH560 (K-ZnO) brought about a dramatic drop in the size of the dispersed phase compared to the case without ZnO. The D_n in the presence of ZnO and K-ZnO were (1.04 ± 0.31) μm and (1.19 ± 0.36) μm, respectively. Thus, the incorporation of ZnO and K-ZnO both resulted in a smaller size and narrower distribution of PBT domains, suggesting finer matrix-dispersed morphology. The morphology of the PA6/PBT/ZnO sample was finer than that of the PA6/PBT/K-ZnO sample, judging from their respective D_n.

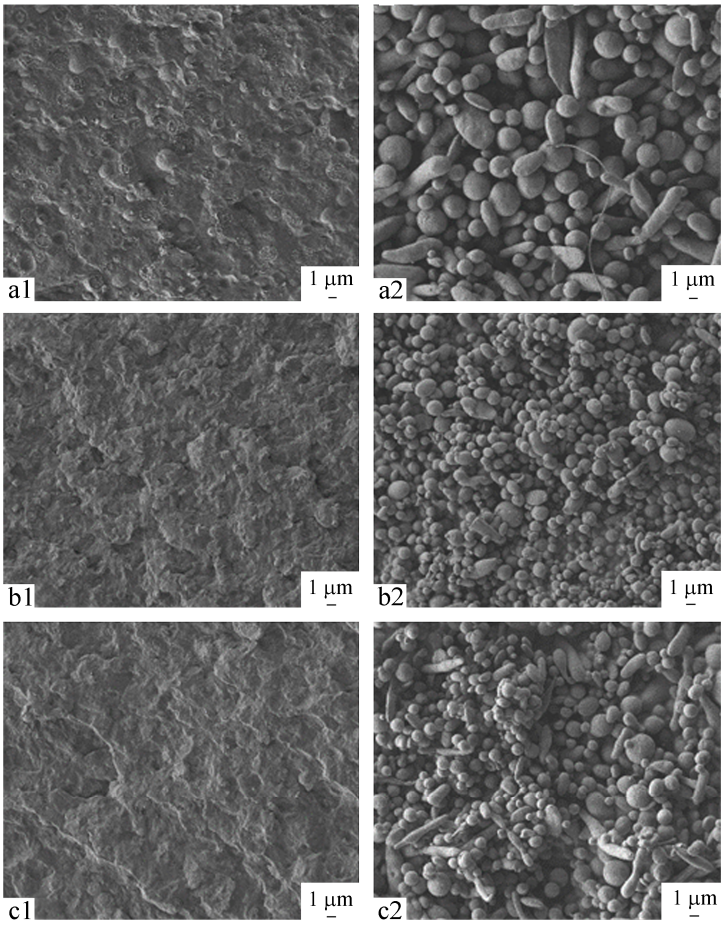


Fig. 1 FESEM micrographs of the cryo-fractured surfaces (a1, b1 and c1) and PBT phases (a2, b2 and c2) of the samples prepared by one-step compounding: (a) PA6/PBT; (b) PA6/PBT/ZnO and (c) PA6/PBT/K-ZnO The PBT phases (a2, b2 and c2) were recovered after selectively etching PA6 phase using formic acid.

Table 2 Statistical results of D_n for all samples

Samples	D_n (μm)
PA6/PBT	1.82 ± 0.57
PA6/PBT/ZnO	1.04 ± 0.31
PA6/PBT/K-ZnO	1.19 ± 0.36
PA6(ZnO)/PBT	1.25 ± 0.35
PA6(K-ZnO)/PBT	1.49 ± 0.47
PA6/PBT(ZnO)	0.98 ± 0.24
PA6/PBT(K-ZnO)	–

PA6 and PBT have similar melting temperatures, which means that the possibilities for ZnO or K-ZnO to interact with PA6 and PBT might be close. Owing to the introduction of epoxy groups onto ZnO after surface modification by KH560, K-ZnO should have high reactivities to the end amine or carboxyl groups of PA6 and PBT molecules. The grafting of both PA6 and PBT chains onto K-ZnO could cause a preferential location of K-ZnO at the interface between PA6 and PBT, which might function as traditional compatibilizer for polymer blends. Unexpectedly, the PA6/PBT/ZnO sample had finer morphology than the PA6/PBT/K-ZnO sample. In order to understand the morphological changes induced by ZnO and K-ZnO, two different compounding sequences in which ZnO or K-ZnO was premixed with one polymer followed by blending with the other polymer were employed. This is believed to change the sequence of the interactions between ZnO or K-ZnO and the two polymers. Figures 2 and 3 present the FESEM micrographs of the samples prepared by the PA6 masterbatch method and PBT masterbatch method, respectively. Compared with the corresponding samples prepared by one-step compounding, the typical matrix-dispersed morphology was retained for the samples prepared by the PA6 masterbatch method, but the size of the dispersed phase increased. The D_n for the PA6(ZnO)/PBT and PA6(K-ZnO)/PBT samples were determined to be (1.25 ± 0.35) and (1.49 ± 0.47) μm, respectively. Similarly, the D_n for the PA6(K-ZnO)/PBT sample was higher than that for the PA6(ZnO)/PBT sample.

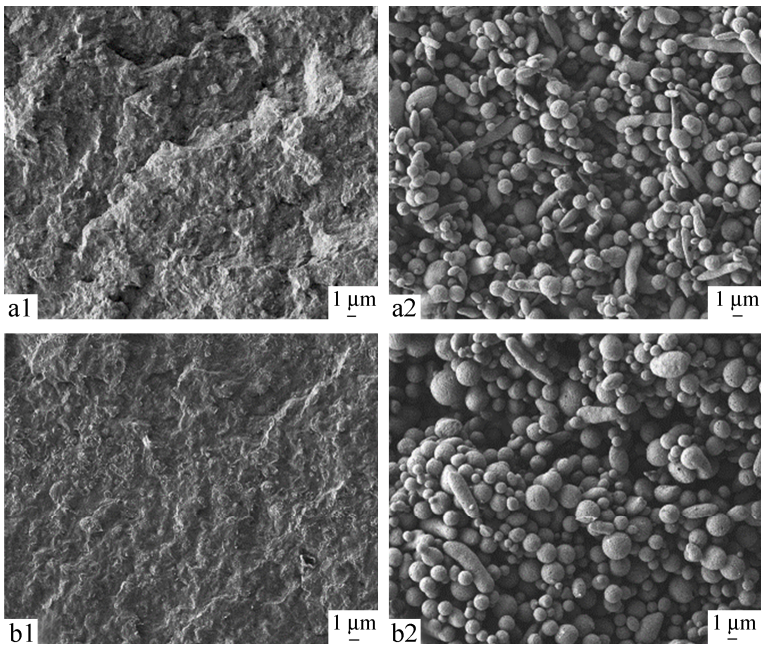


Fig. 2 FESEM micrographs of the cryo-fractured surfaces (a1 and b1) and PBT phases (a2 and b2) of the samples prepared by PA6 masterbatch method: (a) PA6(ZnO)/PBT and (b) PA6(K-ZnO)/PBT
The PBT phases (a2 and b2) were recovered after selectively etching PA6 phase using formic acid.

The morphological changes of the samples prepared by the PBT masterbatch method are more interesting. The PA6/PBT(ZnO) sample still presented typical matrix-dispersed morphology with the D_n being (0.98 ± 0.24) μm, which was even smaller than that of the corresponding sample prepared by one-step compounding. However, when K-ZnO was incorporated, the sample did not lose its integrity after removing PA6 by chemical etching and PBT phase no longer existed as dispersed domains. It can be seen from Fig. 3(b2) that the pores left after chemical etching using formic acid were not closed but interconnected, pointing to co-continuous morphology. The volume fraction of PBT was estimated to be 26% according to the blending composition. Thus, the incorporation of K-ZnO led to special co-continuous morphology at an asymmetric composition when the PBT masterbatch method was utilized.

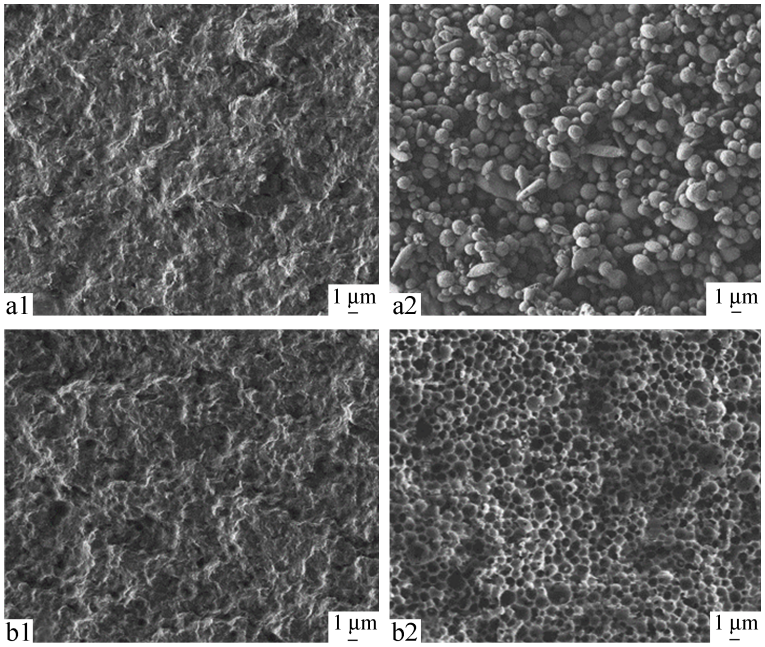


Fig. 3 FESEM micrographs of the cryo-fractured surfaces (a1 and b1) and PBT phases (a2 and b2) of the samples prepared by PBT masterbatch method: (a) PA6/PBT(ZnO) and (b) PA6/PBT(K-ZnO)
The PBT phases (a2 and b2) were recovered after selectively etching PA6 phase using formic acid.

The Dispersion and Distribution States of ZnO and K-ZnO

It has been reported by many researchers that the morphological changes induced by nanoparticles are closely related to their dispersion and distribution states in the incompatible phases. Therefore, the dispersion and location of ZnO and K-ZnO were detected by TEM and the results are shown in Fig. 4. It is not difficult to distinguish PA6 and PBT phases from the TEM micrographs, though the phase contrast between PA6 and PBT is poor. This is because the interfacial zone is lighter, perhaps due to the partial deadhesion between PA6 and PBT phases occurring when preparing the ultrathin slices. Pristine ZnO had a tendency to be distributed preferentially in the PBT phase, whatever compounding sequence was applied. Separated ZnO nanoparticles can be observed and only a few small aggregates (50–100 nm) can be discerned, indicating fairly good dispersion of ZnO in PBT. The situation of K-ZnO is more complex. When one-step compounding was employed, K-ZnO was located partially in PBT and partially at the interface between PA6 and PBT. The location of K-ZnO at the interface must be resulted from a change in the affinity of ZnO to the two phases, which could be ascribed to the reaction between the epoxy groups and the end groups of PA6 chains. When K-ZnO was premixed with PA6, the enrichment of K-ZnO at the interface between PA6 and PBT was more obvious, though a fraction of K-ZnO was still present in the PBT phase. Due to the enrichment of K-ZnO at the interface, the dispersion of K-ZnO was poorer than that of ZnO, considering that many large aggregates of over 200 nm in size circled PBT phase. Compared with one-step compounding, the PA6 masterbatch method provided more time for K-ZnO to interact with PA6, which could cause more PA6 chains to be grafted onto K-ZnO particles. This weakened the affinity of K-ZnO to PBT further, but was still insufficient to prevent all K-ZnO from partitioning into the PBT phase. Thus, most of the incorporated K-ZnO particles were enriched at the interface between PA6 and PBT. When K-ZnO was premixed with PBT, a selective distribution of K-ZnO in the PBT phase was observed. It can be seen from Fig. 4(f) that a thin network of PBT phase encapsulated PA6 phase, which is in agreement with the FESEM observation. Hence, the distribution of ZnO can be adjusted conveniently by changing the surface properties of ZnO and compounding sequences. The controlled structure feature of the PA6/PBT blends with K-ZnO might be employed in the development of functional materials.

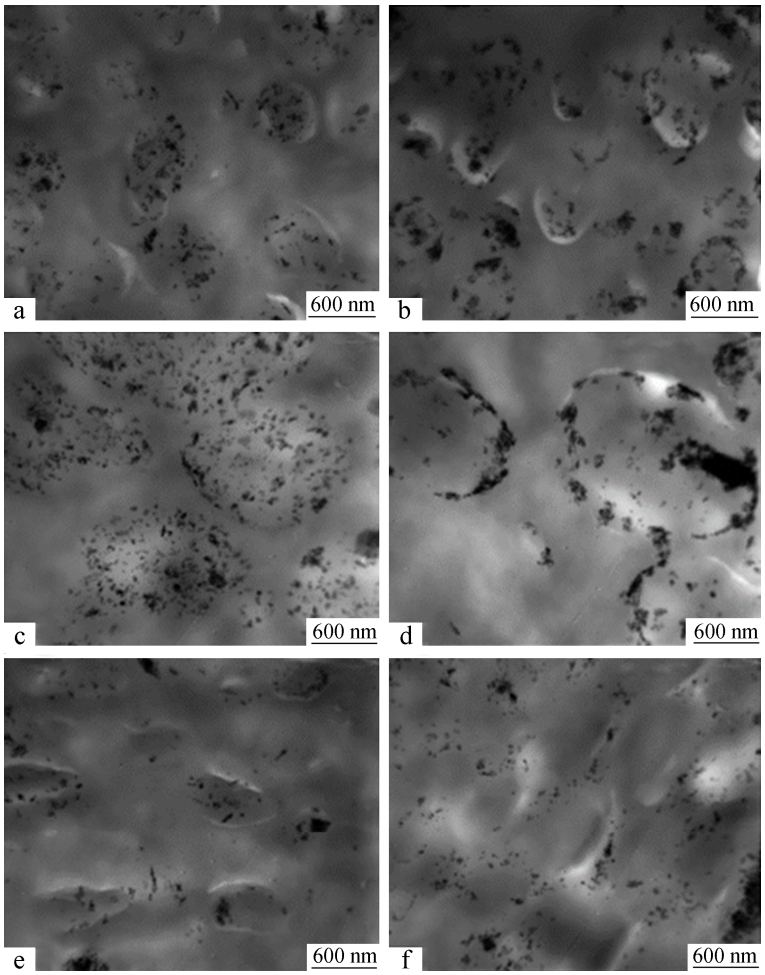


Fig. 4 TEM micrographs of ZnO- and K-ZnO-filled PA6/PBT blends prepared by different compounding sequences: (a) PA6/PBT/ZnO, (b) PA6/PBT/K-ZnO, (c) PA6(ZnO)/PBT, (d) PA6(K-ZnO)/PBT, (e) PA6/PBT(ZnO) and (f) PA6/PBT(K-ZnO)

Mechanism of Morphology Formation

Nanoparticle-induced changes in the viscoelastic properties of blending components and interfacial properties between different phases are two key factors frequently mentioned in interpreting the morphological changes of nanoparticle-incorporated polymer blends. Herein, the influences of ZnO, K-ZnO and KH560 on the viscoelastic properties of PA6 and PBT were evaluated independently. The mixing composition of PA6/ZnO and PA6/K-ZnO was 70/3.09 by weight and that of PBT/ZnO and PBT/K-ZnO was 30/3.09, which are equal to the values listed in Table 1. The weight percentage of KH560 in PA6/KH560 and PBT/KH560 was kept at 1%. The results of dynamic rheological tests are illustrated in Fig. 5. According to a method proposed by Bousmina *et al.*[46], the dynamic rheological values at 10 rad/s were chosen to simulate the actual values in the torque rheometer approximately. The results are summarized in Tables 3 and 4. It can be seen from Fig. 5 that the addition of ZnO caused the complex viscosity-frequency curve to rise slightly at low frequency region but drop modestly at high frequency region, demonstrating more obvious shear-thinning behavior. In addition, a plateau appeared at low frequency region of the storage modulus-frequency curve. These are clear signs that ZnO nanoparticles had achieved rheological percolation state in PA6 melt[18, 47, 48]. In other words, ZnO nanoparticles brought about a confinement effect of adjacent PA6 chains, which would not be broken until high frequency region reached. The dynamic rheological responses of the PA6/K-ZnO melt were similar to those of the PA6/ZnO melt. It should be noted that the complex viscosity and storage modulus of PA6 were enhanced dramatically by the addition of

1 wt% of KH560. At 10 rad/s, the two values increased from 260 Pa·s and 74.3 Pa to 1790 Pa·s and 9280 Pa, respectively. This can be attributed to the chain extension effect of KH560 originating from the reaction between epoxy groups and the end groups of PA6 chains as well as the polymerization of methoxysilane into polysiloxane. Though the situation of mixing PA6 with KH560 is more complicated, it is believed that this provides indirect evidence to the grafting of PA6 chains onto K-ZnO nanoparticles.

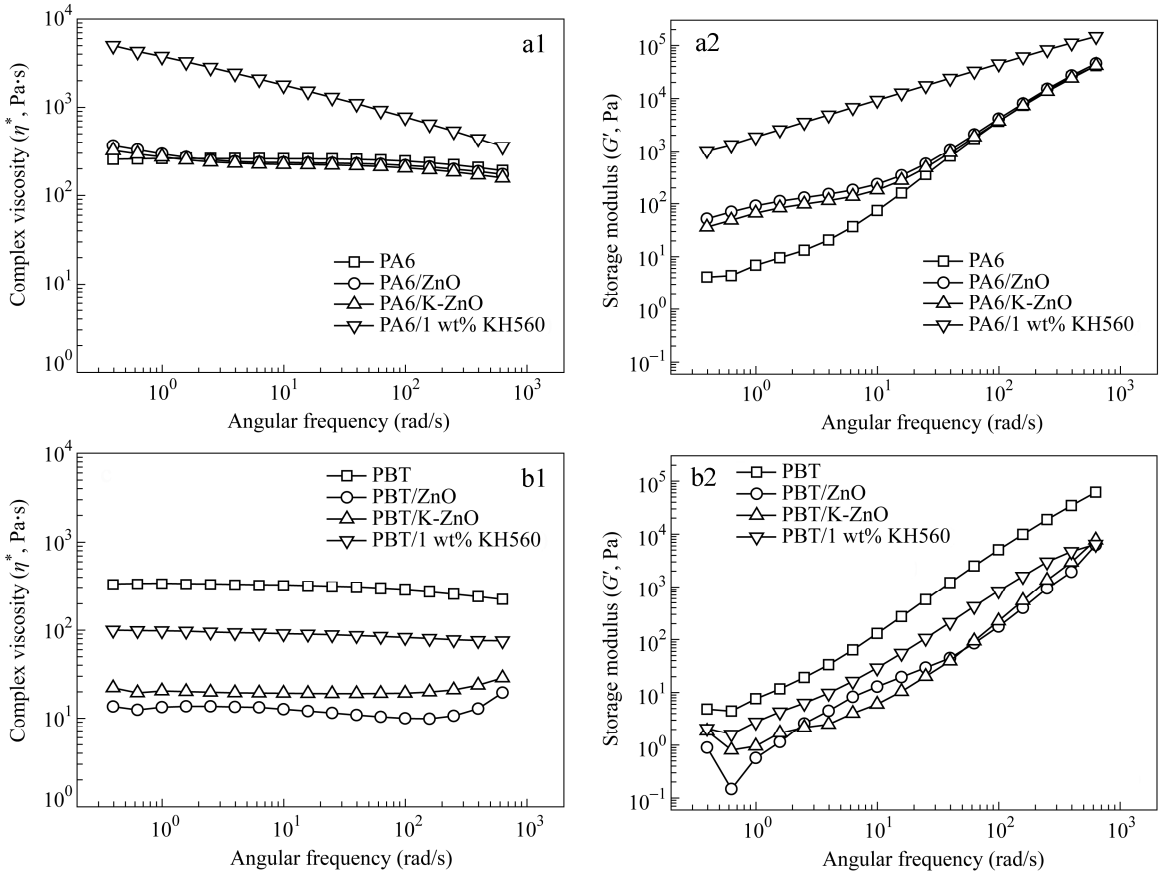


Fig. 5 Plots of complex viscosity (a1 and b1) and storage modulus (a2 and b2) versus angular frequency for PA6 (a1 and a2) and PBT (b1 and b2) filled with ZnO or K-ZnO or mixed with KH560

Table 3 Complex viscosities and storage moduli of PA6 filled with ZnO or K-ZnO or mixed with KH560 at 10 rad/s

	PA6	PA6/ZnO	PA6/K-ZnO	PA6/1 wt% KH560
Complex viscosity (η^*, Pa·s)	260	235	224	1790
Storage modulus (G', Pa)	74	235	183	9280

Table 4 Complex viscosities and storage moduli of PBT filled with ZnO or K-ZnO or mixed with KH560 at 10 rad/s

	PBT	PBT/ZnO	PBT/K-ZnO	PBT/1 wt% KH560
Complex viscosity (η^*, Pa·s)	320	12.7	19.3	91.3
Storage modulus (G', Pa)	130	12.9	6.0	29.2

The complex viscosity and storage modulus of PBT melt were slightly higher than those of PA6 melt. However, the effects of ZnO, K-ZnO and KH560 on the viscoelastic properties of PBT melt were totally different to those of PA6 melt. Dramatic decreases in the complex viscosity and storage modulus of PBT melt were resulted and the decreasing amplitudes followed the order: ZnO > K-ZnO > KH560. This might be due to the degradation in the molecular weight of PBT in the presence of ZnO, K-ZnO or KH560. The ester bonds of

PBT chains have much weaker chemical stability than the amide bonds of PA6 chains, especially under high temperature and intense shear. It has been discovered that basic solids including magnesium oxide (MgO) and ZnO can catalyze the transesterification reaction of esters[49–51]. Moreover, Kim and Kang reported the decrease in the molecular weight of polyesters (poly(ethylene naphthalate) and PBT) resulted from transesterification occurring during reactive blending[52]. Therefore, it is speculated that the transesterification reaction of PBT induced by ZnO, K-ZnO or KH560 may account for the worsened viscoelasticity of PBT. Despite the KH560-induced deterioration in the viscoelastic properties of PBT, the reaction of epoxy groups with the end groups of PBT chains must not be denied. This is because it is well known that epoxy groups have moderate reactivities to carboxyl and hydroxyl groups, which can be accelerated by alkaline compounds. According to the values listed in Tables 3 and 4, the selective distribution of ZnO in the PBT phase would cause a dramatic drop of the complex viscosity ratio between PBT and PA6 from 1.23 to 0.0488, accompanied by a reduction of the storage modulus ratio from 1.75 to 0.173. This may be the reason for the decrease in the size of the dispersed PBT domains induced by ZnO. The pioneering studies of Taylor[53] and Cox[54] have revealed that the deformation and breakup behavior of a liquid droplet in a Newtonian system and under small deformation is closely related to a value named as the capillary number (Ca), defined in the following Eq. (1).

$$\mathrm{Ca}= \eta_{\mathrm{m}} \dot{\gamma} R / \sigma \tag{1}$$

The symbols η_{m}, $\dot{\gamma}$, R and σ represent the viscosity of matrix phase, shear rate, the diameter of droplet and interfacial tension, respectively.

When Ca exceeds a critical value ($\mathrm{Ca_{crit}}$), the effects of shear stress and interfacial tension will lead to the breakup of the droplet. After fitting the plot of the experimental results of Grace[55], Debrujin[56] gave the following Eq. (2) of $\mathrm{Ca_{crit}}$.

$$\lg \mathrm{Ca_{crit}} = -0.506 - 0.0995 \lg p + 0.124 (\lg p)^2 - \frac{0.115}{\lg p - \lg 4.08} \tag{2}$$

The symbol p represents the viscosity ratio between dispersed phase and matrix phase. By substituting the complex viscosity ratio calculated in our work into Eq. (2), an increase of $\mathrm{Ca_{crit}}$ from 0.509 to 0.790 after the addition of ZnO is obtained. This indicates that the critical diameter of droplets that can break up is increased, thus is not beneficial to the formation of finer morphology. Hence, the viscosity ratio change caused by ZnO is not the reason for the morphological change. Here it is believed that the ZnO-induced drop in the molecular weight of PBT will raise the number of end carboxyl groups of PBT. Meanwhile, ZnO can catalyze ester-amide exchange reaction between PBT and PA6 molecules. Both effects may improve the compatibility between PBT and PA6, thus leading to the drop in the size of the dispersed phase. Lin *et al.*[51] reported the compatibilization of PBT/PC by *in situ* formed copolymers produced by MgO-catalyzed transesterification, which supports our speculation. From this point of view, the differences in D_n of the ZnO-filled PA6/PBT blends prepared by different compounding sequences were due to different extents of transesterification and ester-amide exchange reactions.

The K-ZnO-filled PA6/PBT blends prepared by one-step compounding and the PA6 masterbatch method demonstrate different extents of enrichment of K-ZnO at the interface. The K-ZnO particles located at the interface with dual grafting of PA6 and PBT can function as traditional compatibilizer in refining blend morphology. On one hand, they can reduce the interfacial tension between PA6 and PBT, promoting the breakup of PBT phase effectively. On the other hand, they can suppress the coalescence of dispersed droplets, as have been reported by many researchers in organoclay-filled polymer blends[4, 5, 12]. Nevertheless, less K-ZnO nanoparticles were distributed in PBT for the PA6/PBT/K-ZnO and PA6(K-ZnO)/PBT samples, leading to lower extents of transesterification. These two factors can exert contrary effects in morphology formation. The results listed in Table 1 show that the D_n of K-ZnO-filled samples were higher than the corresponding ZnO-filled samples and the D_n of the PA6(K-ZnO)/PBT sample was larger than that of the PA6/PBT/K-ZnO sample. Judging from this, it can be predicted that the transesterification of PBT induced by K-ZnO dominated over the interfacial effect of K-ZnO in influencing morphology formation.

It is difficult to understand the co-continuous morphology of the PA6/PBT(K-ZnO) sample, considering that the PA6/PBT(ZnO) sample still retained matrix-dispersed morphology and the influences of ZnO and K-ZnO on the viscoelasticity properties of PBT melt were quite similar. According to the equations predicting the phase inversion composition of polymer blends[1], the viscosity ratio drop induced by ZnO and K-ZnO was beneficial to the occurrence of phase inversion and the formation of matrix-dispersed morphology with PBT as matrix. It was believed that the compatibilizing effect of K-ZnO helped to stabilize the intermediate co-continuous morphology formed during blending.

Rheological Properties

Herein, an important question arises how the different structural features caused by ZnO and K-ZnO in different compounding sequences affect the final properties of PA6/PBT blends. The complex viscosities and storage moduli of the samples were determined in melt rheological tests. The results are compared in Fig. 6 and Table 5. It can be seen that the complex viscosity and storage modulus curves of the samples with pristine ZnO are all below the corresponding curves of the PA6/PBT sample. For instance, the highest complex viscosity and storage modulus of the samples with pristine ZnO at 10 rad/s are 97.6 Pa·s and 301 Pa, which are lower than the corresponding values of the PA6/PBT sample (180 Pa·s and 410 Pa). Similar results were obtained when the melt rheological tests were conducted repeatedly. Therefore, this is due to the detrimental effect of ZnO on the viscoelastic properties of PBT rather than experimental error. In sharp contrast, no obvious reduction is observed for the PA6/PBT/K-ZnO and PA6(K-ZnO)/PBT samples. The complex viscosity and storage modulus curves of the two samples even lie above the corresponding curve of the PA6/PBT sample at low frequency region.

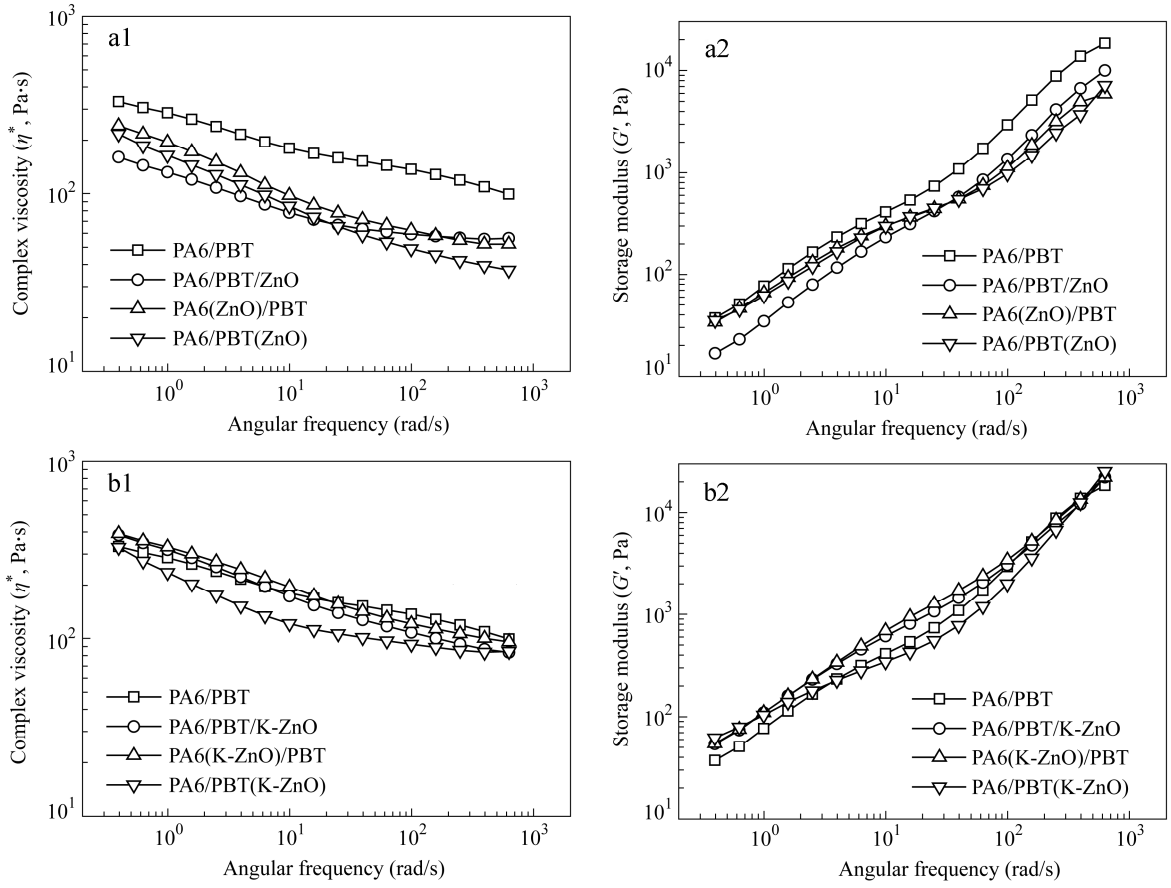


Fig. 6 Plots of complex viscosity (a1 and b1) and storage modulus (a2 and b2) versus angular frequency for ZnO (a1 and a2) and K-ZnO (b1 and b2) -filled PA6/PBT blends prepared by different compounding sequences

Table 5 Complex viscosities and storage moduli of ZnO- and K-ZnO-filled PA6/PBT blends prepared by different compounding sequences at 10 rad/s

Samples	Complex viscosity (η^*, Pa·s)	Storage modulus (G', Pa)
PA6/PBT	180	410
PA6/PBT/ZnO	78	232
PA6(ZnO)/PBT	98	301
PA6/PBT(ZnO)	85	298
PA6/PBT/K-ZnO	173	610
PA6(K-ZnO)/PBT	195	689
PA6/PBT(K-ZnO)	121	343

Moreover, the complex viscosity of the PA6(K-ZnO)/PBT sample is slightly higher than that of the PA6/PBT/K-ZnO over the whole frequency region. It can be seen from Table 5 that the storage modulus of the PA6(K-ZnO)/PBT sample at 10 rad/s is 689 Pa, which is 68% higher than that of the PA6/PBT sample. These all point to a deduction that the enrichment of K-ZnO at the interface can facilitate the shear stress transfer from PA6 to PBT. Meanwhile, the harmful effect of K-ZnO on the viscoelastic properties of PBT can be depressed when less K-ZnO was distributed in PBT.

Therefore, ZnO nanoparticles can be enriched at the interface between PA6 and PBT by surface modification using KH560 and changing compounding sequences, which can enhance the viscoelastic properties of the PA6/PBT blend substantially.

CONCLUSIONS

Both ZnO and K-ZnO can bring about a smaller size and narrower distribution of PBT domains for PA6/PBT (70/30, *W*/*W*) blend in one-step compounding and the effect of ZnO is greater than K-ZnO. Two-step compounding in which ZnO or K-ZnO was premixed with PA6 or PBT has been compared and mixing PA6 with premixed PBT/ZnO yields finest morphology. ZnO is selectively distributed in PBT phase, while K-ZnO tends to be enriched at the interface except when K-ZnO is premixed with PBT. ZnO and K-ZnO can lower the molecular weight of PBT, which produces more end carboxyl groups and improves the compatibility between PA6 and PBT. This accounts for the refined morphology of PA6/PBT blend. The viscoelastic properties of the PA6/PBT blend can be enhanced substantially with interfacially localized K-ZnO. Therefore, the present study obtains refined morphology, well-controlled structure features and enhanced properties of PA6/PBT blend by incorporating K-ZnO and changing compounding sequences, which may be of great value in developing new materials with high performance and advanced functions.

REFERENCES

1 Macosko, C.W., Macromol. Symp., 2000, 149(1): 171
2 Wang, Y., Zhang, Q. and Fu, Q., Macromol. Rapid Commun., 2003, 24(3): 231
3 Khatua, B.B., Lee, D.J., Kim, H.Y. and Kim, J.K., Macromolecules, 2004, 37(7): 2454
4 Das, A.K., Suin, S., Shrivastava, N.K., Maiti, S., Mishra, J.K. and Khatua, B.B., Polym. Compos., 2014, 35(2): 273
5 Chandran, N., Chandran, S., Maria, H.J. and Thomas, S., RSC Adv., 2015, 5(105): 86265
6 Elias, L., Fenouillot, F., Majesté, J.C., Alcouffe, P. and Cassagnau, P., Polymer, 2008, 49(20): 4378
7 Liu, X.Q., Wang, Y., Yang, W., Liu, Z.Y., Luo, Y., Xie, B.H. and Yang, M.B., J. Mater. Sci., 2012, 47(11): 4620
8 Wu, D.F., Zhang, Y.S., Zhang, M. and Yu, W., Biomacromolecules, 2009, 10(2): 417
9 Bose, S., Bhattacharyya, A.R., Kodgire, P.V., Misra, A. and Pötschke, P., J. Appl. Polym. Sci., 2007, 106(5): 3394
10 Hrnjak-Murgić, Z., Jelčić, Ž., Kovačević, V., Mlinac-Misăk, M. and Jelenčić, J., Macromol. Mater. Eng., 2002, 287(10): 684
11 Jiang, L., Liu, B. and Zhang, J.W., Ind. Eng. Chem. Res., 2009, 48(16): 7594
12 Li, Y.J. and Shimizu, H., Macromol. Rapid Commun., 2005, 26(9): 710

13 Zhang, B.Q., Ding, Y.F., Chen, P., Liu, C.Y., Zhang, J., He, J.S. and Hu, G.H., Polymer, 2005, 46(14): 5385
14 Filippone, G., Dintcheva, N.T., Acierno, D. and Mantia, F.P.L., Polymer, 2008, 49(5): 1312
15 Kong, M.Q., Huang, Y.J., Chen, G.L., Yang, Q. and Li, G.X., Polymer, 2011, 52(22): 5231
16 Lee, S.H., Kontopoulou, M. and Park, C.B., Polymer, 2010, 51(5): 1147
17 Laoutid, F., François, D., Paint, Y., Bonnaud, L. and Dubois, P., Macromol. Mater. Eng., 2013, 298(3): 328
18 Zou, H., Wang, K., Zhang, Q. and Fu, Q., Polymer, 2006, 47(22): 7821
19 Xiang, F.M., Shi, Y.Y., Li, X.X., Huang, T., Chen, C., Peng, Y. and Wang, Y., Eur. Polym. J., 2012, 48(2): 350
20 Zhang, L.Y., Wan, C.Y. and Zhang, Y., Compos. Sci. Technol., 2009, 69(13): 2212
21 Chen. J., Chen, P., Wu, L., Zhang, J. and He, J.S., Polymer, 2006, 47(15): 5402
22 Paran, S.M.R., Naderi, G. and Ghoreishy, M.H.R., Appl. Surf. Sci., 2016, 382: 63
23 Nofar, M., Heuzey, M.C., Carreau, P.J. and Kamal, M.R., Polymer, 2016, 98(SI): 353
24 Mallakpour, S. and Nouruzi, N., J. Mater. Sci., 2016, 51(13): 6400
25 Huang, S.J., Bai, L., Trifkovic, M., Cheng, X. and Macosko, C.W., Macromolecules, 2016, 49(10): 3911
26 Durandish, M. and Alipour, A., Chinese J. Polym. Sci., 2013, 31(4): 660
27 Lin, C.Y., Zuo, M., Lin, H.H., Liu, T. and Zheng, Q., Chinese J. Polym. Sci., 2015, 33(8): 1162
28 Hong, R.Y., Chen, L.L., Li, J.H., Li, H.Z., Zheng, Y. and Ding, J., Polym. Adv. Technol., 2007, 18(11): 901
29 Yu, W., Lan, J.H., Wang, S.J., Fang, P.F. and Sun, Y.M., Polymer, 2010, 51(11): 2403
30 Jose, J.P., Chazeau, L., Cavaillé, J.Y., Varughese, K.T. and Thomas, S., RSC Adv. 2014, 4(4): 31643
31 Peng, G.R., Li, Q.S., Yang, Y.L. and Wang, H.F., J. Appl. Polym. Sci., 2009, 114(4): 2128
32 Cao, W., Zhou, B., Liu, Y.H., Ma, X.Y., Liu, Y., Wang, Z.C. and Zhu, Y.C., Polym. Int., 2013, 62(3): 432
33 Wong, M.H., Guenther, J., Sun, L.Y., Blümel, J., Nishimura, R. and Sue, H.J., Adv. Funct. Mater., 2012, 22(17): 3614
34 Therias, S., Larché, J.F., Bussière, P.O., Gardette, J.L., Murariu, M. and Dubois, P., Biomacromolecules, 2012, 13(10): 3283
35 Díez-Pascual, A.M. and Díez-Vicente, A.L., ACS Appl. Mater. Interfaces, 2014, 6(13): 10132
36 Díez-Pascual, A.M. and Díez-Vicente, A.L., ACS Appl. Mater. Interfaces, 2014, 6(5): 3729
37 Murariu, M., Doumbia, A., Bonnaud, L., Dechief, A.L., Paint, Y., Ferreira, M., Campagne, C., Devaux, E. and Dubois, P., Biomacromolecules, 2011, 12(5): 1762
38 Ding, J.W., Zhu, S.Y., Zhu, T., Sun, W., Li, Q., Wei, G. and Su, Z.Q., RSC Adv., 2015, 5: 22935
39 Scaffaro, R., Botta, L., La Mantia, F.P., Gleria, M., Bertani, R., Samperi, F. and Scaltro, G., Polym. Degrad. Stab., 2006, 91(10): 2265
40 Jeziórska, R., Polym. Degrad. Stab., 2005, 90(2): 224
41 van Dubin, M., van Gurp, M., Leemans, L., Walet, M., Aussems, M., Martin, P., Legras, R., Machado, A.V. and Covas, J.A., Macromol. Symp., 2003, 198(1): 135
42 Lievana, E. and Karger-Kocsis, J., Macromol. Symp., 2003, 202(1): 59
43 Kim, S.J., Kim, D.K., Cho, W.J. and Ha, C.S., Polym. Eng. Sci., 2003, 43(6): 1298
44 Wang, L., Guo, Z.X. and Yu, J., Ind. Eng. Chem. Res., 2014, 53(1): 206
45 Zeng, Z., Yu, J. and Guo, Z.X., Macromol. Chem. Phys., 2004, 205(16): 2197
46 Bousmina, M., Ait-Kadi, A. and Faisant, J.B., J. Rheol., 1999, 43(2): 415
47 Cheng, H.K.F., Sahoo, N.G., Pan, Y.Z., Li, L., Chan, S.H., Zhao, J.H. and Chen, G., J. Polym. Sci., Part B: Polym. Phys., 2010, 48(11): 1203
48 Médéric, P., Razafinimaro, T., Aubry, T., Moan, M. and Klopffer, M.H., Macromol. Symp., 2005, 221(1): 75
49 Bancquart, S., Vanhove, C., Pouilloux, Y. and Barrault, J., Appl. Catal. A: Gen, 2001, 218(1-2): 1
50 Ferretti, C.A., Olcese, R.N., Apesteguía, C.R. and Cosimo, J.I.D., Ind. Eng. Chem. Res., 2009, 48(23): 10387
51 Lin, G.P., Lin, L., Wang, X.L., Chen, L. and Wang, Y.Z., Ind. Eng. Chem. Res., 2015, 54(4): 1285
52 Kim, H. and Kang, H.J., Polym. Korea, 2006, 30(1): 22
53 Taylor, G.I., Proc. R. Soc. Lond. A, 1934, 146(858): 501
54 Cox, R.G., J. Fluid Mech., 1969, 37(3): 601
55 Grace, H.P., Chem. Eng. Commun., 1982, 14(3-6): 225
56 Debrujin, R.A., Dissertation, The Netherlands: Eindhoven University of Technology, 1989